Contents lists available at ScienceDirect

International Journal of Electrochemical Science

Synthesis, structural characterisations, electrochemical behavior and antibacterial activities of a chromium(III) resorcinolate complex

Tigist Tsega [a], Getasil Chanie [a], Adane Kassa [e], Mamo Gebrezgiabher [b,c], Dawit Tesfaye [b,c], Melaku Metto [a], Mamaru Bitew [e], Getinet Tamiru Tigineh [a], Wolfgang Linert [d], Madhu Thomas [b,c,*], Atakilt Abebe [a,**]

[a] Department of Chemistry, College of Science, Bahir Dar University, P.O.Box 79, Bahir Dar, Ethiopia
[b] Department of Industrial Chemistry, College of Natural and Applied Sciences, Addis Ababa Science and Technology University, P.O. Box 16417, Addis Ababa, Ethiopia
[c] Nanotechnology Centre of Excellence, Addis Ababa Science and Technology University, P.O. Box 16417, Addis Ababa, Ethiopia
[d] Institute of Applied Physics, Vienna University of Technology, Wiedner Hauptstraße 8-10, Vienna 1040, Austria
[e] Department of Chemistry, College of Natural and Computational Sciences, Debre Markos University, P.O.Box 269, Ethiopia

ARTICLE INFO

ABSTRACT

The integration and implementation of transition metal complexes as working electrode for surface modifications has become an area of research interest now a days. Based on this, a novel anionic complex having a formula of $Na_3[Cr(HR)_4Cl_2]$ (HR^- = resorcinolate) with octahedral geometry, was prepared and characterized by elemental analysis, molar conductance, vibrational spectra. Electropolymerization of the ligand, salt, and complex was done on glassy carbon electrodes with effective surface area 0.15, 0.17, and 0.2 cm^2 for poly(NaHR)/GCE, Cr(0)/GCE, and poly($Na_3[Cr(HR)_4(Cl_2)]$)/GCE respectively. The presence of a redox polymer film on the surface of the electrode was indicated by the experimental changes observed for a solution containing $Na_3[Cr(HR)_4Cl_2]$. Specifically, the anodic peak currents, which represent the oxidation process, showed significant increases at different potential values compared to the ligand and salt. These potential values were approximately + 114 mV and + 573 mV. Additionally, the cathodic peak current, which is corresponding to the reduction process, exhibited changes at − 230 mV as the scan cycles were increased. These variations strongly suggested the formation of a film composed of a redox polymer on the electrode's surface. Further, the resistance to charge transfer (Rct) of the compound is in the lower voltage compared to the free ligand, $CrCl_3 \bullet 6H_2O$, and the unmodified GCE. This indicates that the modified compound exhibits improved conductivity due to its reduced charge transfer resistance. The antibacterial activity assessed against two Gram-positive bacteria strains (*Staphylococcus aureus* and *Streptococcus epidermis*) and two Gram-negative bacteria strains (*Escherichia coli* and *Klebsiella pneumoniae*), indicate that the Cr(III) complex exhibit higher antibacterial activity compared to the ligand and the metal salt but lower than the reference. The synthesized is a highly conductive material suitable for potential applications in sensors and catalysis, especially in situations that require efficient and rapid electron transfer process

1. Introduction

The superiority of metal complexes over the corresponding metal salts and ligands make them suitable candidates for material development, such as electrode surface modifiers for sensing applications and metal-based drugs. Modified electrodes with alterations at the molecular level are employed in electron transfer In this respect, coordination chemistry of chromium have attracted the attention of many investigators due its versatile complex formation and electrochemical behaviour [1–4]. The electrochemistry of chromium(III) complexes has shown increasing interest due to the wide range of oxidation states of chromium and excellent electrochemical redox characteristics [5,6] and is crucial metal for electrochemical catalytic reactions [7]. The electrocatalytic capability of chromium(III) complexes have been

investigated also for potential applications in energy storage systems [8–11].

Moreover, chromium(III) complexes are considered less toxic and more environmentally friendly than chromium(VI) that they have been explored for their therapeutic application as potential drug candidates [12,13] and there are reports on the antibacterial, antifungal, and anticancer activities of chromium(III) complexes [14–16]. Additionally, it has been observed that these complexes can influence glucose, fat, and protein metabolism and thus potentially enhancing the effects of insulin [17–19]. Chromium(III) also contributes to lipid metabolism, reducing the risk of atherogenesis [20], promoting lean body mass [21], and aiding the weight loss [22].

Here in, we have prepared chromium(III) complex of resorcinol and characterised by various physic-chemical techniques. The complex is further explored for its electrochemaical behaviour by cyclic voltammetry and electroscopic and antibacterial activities.

2. Experimental

2.1. Chemicals and solvents

Hydrated chromium chloride ($CrCl_3.6H_2O$) (98 %, Blulux laboratories), resorcinol ($C_6H_6O_2$) (99.0 %, HI Media Laboratories), silver nitrate (99.9 %, Sigma Aldrich), Muller-Hinton agar (oxoid Ltd Basingstok, England), potassium bromide (Blulux laboratories), sodium hydroxide (Sigma Aldrich), and triethanolamine (98 %) (Sigma Aldrich) were used without any further purifications.

Solvents such as DMSO (99.0 %, Loba Chemie.), DMF (99.9 %, Carlo Erba reagents), ethanol (HI Media Laboratories), THF (99.8 %, Loba Chem,), methanol (99.5 %, Loba Chem), acetone (99.8 %, Carlo Erba reagent), chloroform (99.99 %, Fisher Scientific UK), dichloromethane (99.5 %, Loba Chem), acetonitrile (99.9 %, Sigma Aldrich) and distilled water were also used in the present investigations.

2.2. Instruments and analyses

Metal and halide content were determined by the standard methods [23]. Molar conductivity of the complex was measured using a 10^{-3} M methanol solution at room temperature using an Adwa, AD 8000, pH/mv/EC/TDS meter. The FTIR spectra were obtained in PerkinElmer L1 600 400 Spectrum in the region 4000–400 cm^{-1} in potassium bromide pellets. The Uv-vis in the 200–800 nm range were collected in distilled water on a DR6000 UV/Vis spectrophotometer. CHI 760E Electrochemical Workstation (Austin, Texas, USA) was used to assess the electrochemical nature of the complex. The antibacterial test was performed on two Gram-positive bacteria (*S. aureus* and *S. epidermidis*) and two Gram-negative bacteria (*E. coli* and *K. pneumonia*) on Muller-Hinton agar media and tetracycline as the standard drug.

2.3. Synthesis of NaHR

Aqueous solution of NaOH (0.072 g, 1.8 mmol), 30 mL was slowly added to 30 mL aqueous solution of resorcinol (0.2 g, 1.8 mmol) under stirring at room temperature.It is further stirred for 1 more hour. From the resultant yellowish solution so obtained, was dried under reduced pressure. The brown solid separated was dried under vacuum over $CaCl_2$ (yield: 0.21 g, 87.5 %) (Scheme 1).

2.4. Synthesis of $Na_3[Cr(HR)_4Cl_2]$

A solution of NaHR in ethanol (0.18 g, 30 mL) was added to an ethannolic solution of $CrCl_3·6H_2O$ (0.1 g, in 30 mL) under stirring. The resultant solution was refluxed at 120 °C for 5 h and cooled to room temperature.From the brownish-green solution resulted, the solvent was evaporated under reduced pressure, yielded a dark green powder. It was then recrystallized from ethanol and dried in air (yield: 0.23 g (88.50 %) (Scheme 1).

3. Results and discussions

3.1. Physico-chemical characterizations

The complex $Na_3[Cr(HR)_4Cl_2]$ is dark green in colour and is soluble in water, methanol, dimethyl sulfoxide and ethanol and insoluble in chloroform, acetonitrile, dimethylformamide, tetrahydrofuran, dichloromethane, and acetone. The elemental analysis data reveal that the complex can be represented as $Na_3Cr(HR)_4Cl_2$. The electrical conductivity of the complex in MeOH (10^{-3} M) is 301 ohm^{-1} cm^2 mol^{-1} prove a 1:3 conducting nature [24]. Thus, the complex can be formulated as $Na_3[Cr(HR)_4Cl_2]$. Found: Cr - 4.20 %, Na - 11.00 % and Cl - 11.20 %; Calculated for $Na_3CrC_{24}H_{20}O_8Cl_2$: Cr - 4.20 %, Na - 10.80 % and Cl - 11.20 %.

3.2. FT-IR spectra

Infrared spectrum of resorcinol, its sodium derivative and the corresponding chromium complex are shown in Fig. S2. The νO-H band of the free ligand at 3258 cm^{-1} shifted to 3446 cm^{-1} in NaHR and 3429 cm^{-1} in $Na_3[Cr(HR)_4Cl_2]$Cl. The stretching vibration of νC=C of resorcinol at 1609 cm^{-1} is shifted to 1636 cm^{-1} in the complex, confirming coordination [25]. A new band appeared at 512 cm^{-1}, assigned to νCr-O, further supporting the coordination of the phenolate group in the deprotonated condition.

3.3. UV-Visible spectra

The electronic spectra of the ligand, salt, and complex were compared to determine changes in the electronic environment and assist in structure elucidation (Fig. S1). In the ligand spectra, bands
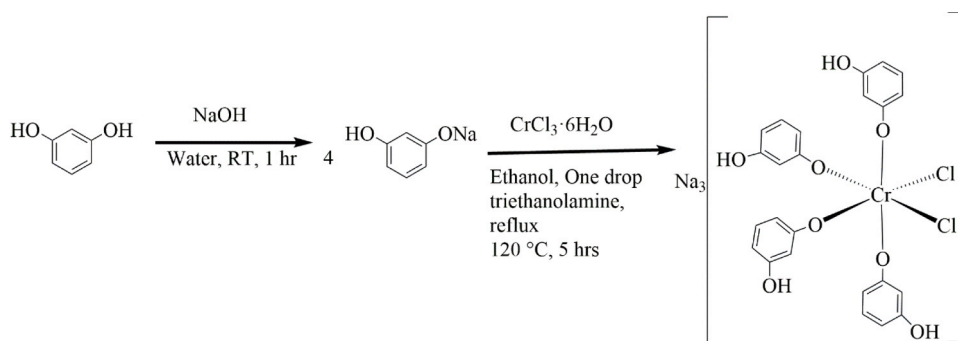
Scheme 1. Synthetic route for the preparation of the complex $Na_3[Cr(HR)_4Cl_2]$.

corresponding to π →π* (C═C) and n→σ* (C-O) transitions were observed at 273 nm and, 215 nm respectively. On coordination, these bands shifted to 280 nm and 340 nm, indicating a change in the ligand's electronic environment. Additionally, a new band appeared at 490 nm in the complex's spectrum, corresponding to ($^4A_{2g}(F) \rightarrow {}^4T_{2g}(F)$) transition (Fig. S1) [26]. suggesting an octahedral geometry around Cr(III) ion [27].

3.4. Electrochemical characterizations

3.4.1. Cyclic voltammetry

In the cyclic voltammetric studies, formation and disappearance of cathodic and anodic peaks, as well as differences in peak current intensity, are the evidences of the transformation of the salt and ligands into the corresponding complex [28].

Fig. 1 illustrates the formation of a polymer layer on the glassy carbon electrode (GCE) surface using a solution containing sodium resorcinolate (NaHR), $CrCl_3 \cdot 6H_2O$, and $Na_3[Cr(HR)_4Cl_2]$. The cyclic voltammograms show an increase in peak current for the anodic peaks centered around + 357 mV and + 1354 mV, and the cathodic peak at − 1544 mV in the presence of resorcinolate. The electrodeposited chromium(0) peak current were observed at + 1116 mV (anodic) and − 327 mV (cathodic). The synthesized complex exhibited increased peak current for the anodic peaks centered around + 114 mV and + 573 mV, and the cathodic peak at − 230 mV with increasing scan cycles, indicating the formation of a redox polymeric film on the electrode surface.

The disappearance of certain cathodic peaks (labeled as "a" in $CrCl_3 \cdot 6H_2O$) and (labeled as "b" for resorcinolate) after coordination indicates the binding of resorcinolate and the formation of $Na_3[Cr(HR)_4Cl_2]$. The proposed mechanism of the electropolymerization of the synthesized complex on the surface of the electrode is shown in Scheme 2. The double bonds on the aromatic carbon initiates the formation of polymer by forming radical cation. The radical easily propagates the continuous bonding with the successive monomer, by potentiodynamic polymerization.

Ferricyanide is mentioned as a commonly used redox-active species in electrochemical studies. It is employed to raise the redox potential of solutions, act as a potential standard, and facilitate electron transfer in electrochemical cells. Glassy carbon electrodes are frequently used in electrochemical processes, and their modification can involve mixing various components [29]. The electro-polymerization tendencies of the compounds on the GCE are depicted in Fig. 2. Cyclic voltammetry curves of $Fe(CN)_6^{3-/4-}$ on various forms of GCE, the presence of redox peaks indicate the successful modification of the electrodes [30]. The potential separation (ΔEp) of anodic and cathodic peaks suggests a quasi-reversible reaction [31]. Increasing the scan rate leads to shifts in the peak potentials, indicating effective mass transfer between the electrodes [32].

The slope of the plot of anodic peak current vs. the square root of the scan rate is directly proportional to the effective surface area of the electrode according to the Randles Sevcik equation ((1)) [33]. A higher
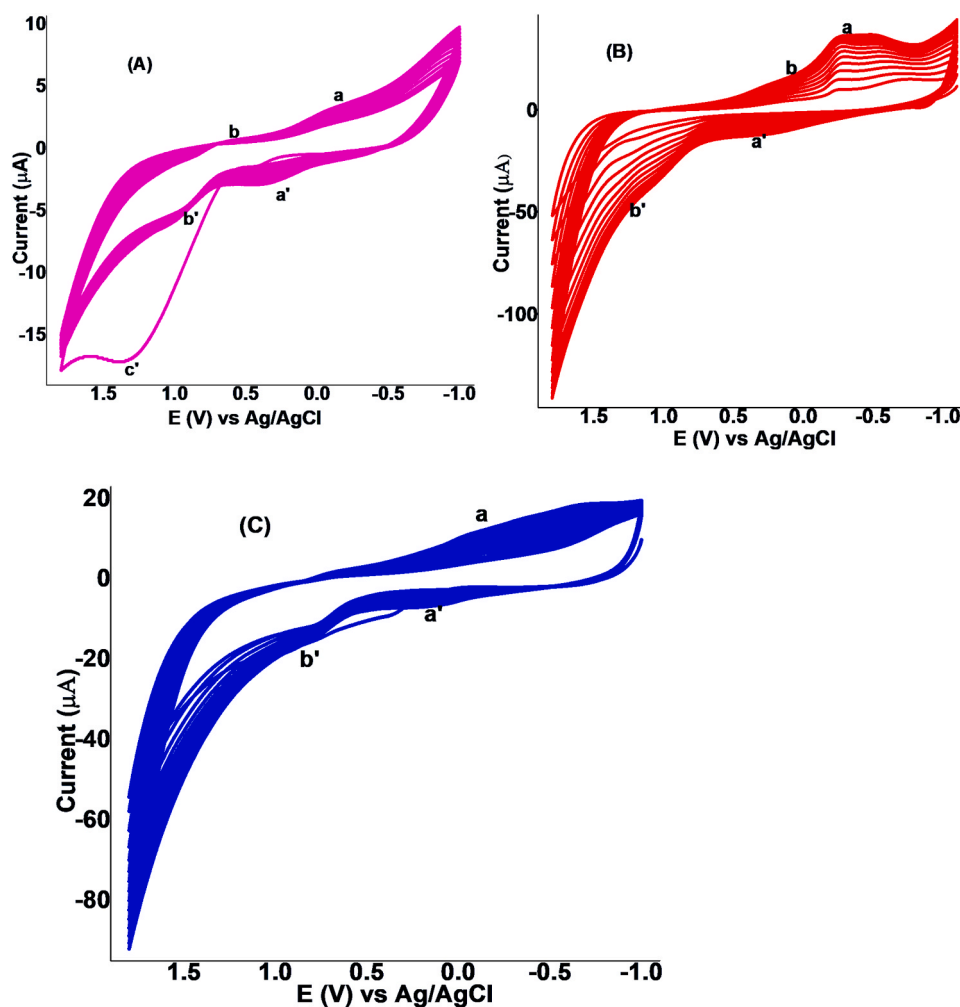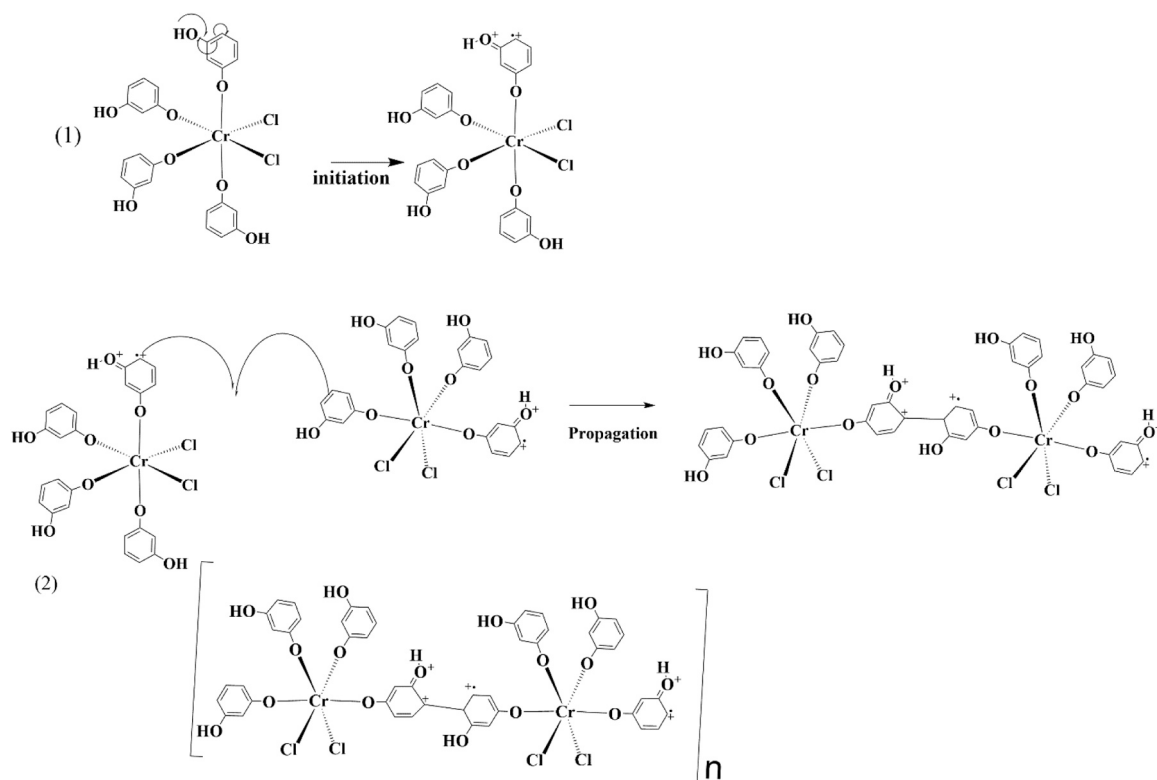

Fig. 1. The CV of PBS (pH 7.0) containing 1.0 mM NaHR (A), $CrCl_3.6H_2O$ (B), and $Na_3[Cr(HR)_4Cl_2]$ (C) scanned on the surface of GCE at a scan rate of 100 mV s^{-1} for 15 cycles in the potential window of -1.0 to 1.9 V.

Scheme 2. The proposed mechanism for the electropolymerization.

slope value for the newly synthesized complex suggests a larger surface area compared to the ligand and $CrCl_3.6H_2O$. The surface area, slope, conductivity, and stability of a complex are interrelated and can impact its performance in various applications as presented in Table 1 [34].

$$I_p = 2.69x10^5AD^{1/2}n^{3/2}Cv^{1/2} \tag{1}$$

Where I_p = Peak current (amperes), **n** is the Number of electrons transferred in a redox cycle, **A** is the electrode surface area (cm^2), **C** is the molar concentration of redox-active species (mol/cm^3), **D** is the diffusion coefficient (cm^2/s), **v** is scan rate in V/s.

$Na_3[Cr(HR)_4Cl_2]$ with redox-active properties can undergo redox reactions, generating reactive oxygen species (ROS) that can damage bacterial cells and exhibit antibacterial activity. The electrochemical characteristics of a complex, such as the potential gap between the HOMO and LUMO, can influence its stability and ability to interact with bacterial membranes.

Fig. 3 demonstrate, the potential gap of $Na_3[Cr(HR)_4Cl_2]$ is higher than the potential gap of the ligand and $CrCl_3.6H_2O$. This suggests that $Na_3[Cr(HR)_4Cl_2]$ has a larger energy difference between its HUMO and LUMO, indicating potentially increased stability compared to the NaHR and $CrCl_3.6H_2O$.

The peak-to-peak separation between poly(NaHR)/GCE and poly($Na_3[Cr(HR)_4Cl_2]$)/GCE is smaller, indicating that the poly($Na_3[Cr(HR)_4Cl_2]$)/GCE undergoes a smaller change in potential during the redox process compared to the poly(NaHR)/GCE. It is notable that, the peak-to-peak separation of the poly(Cr(0)/GCE, poly($Na_3[Cr(HR)_4Cl_2]$)/GCE is higher, suggesting a larger potential change during the redox process.

Poly($Na_3[Cr(HR)_4Cl_2]$)/GCE (curve a) displays a cathodic peak potential of 0.054 V at 151.9 μA and an anodic peak potential of 0.191 V at -111 μA. The ligand (curve b) exhibits an anodic peak potential at 0.182 V at -99.62 μA and a cathodic peak potential at 0.055 V at 142.9 μA. The poly(Cr(0))/GCE (curve c) exhibits a cathodic peak potential at 0.044 V at 66.47 μA and an anodic peak potential at -36.75 μA

at 0.173 V.

The electro-active surface area of poly($Na_3(Cr(HR)_4Cl_2]$)/GCE (0.2 cm^2) is higher than that of the unmodified GCE (0.069 cm^2). The significant enhancement in electro-active surface area of the modified electrode is the evidence for the formation of a larger number of available electrochemical active sites on the surface of poly($Na_3(Cr(HR)_4Cl_2]$)/GCE which offers more electrocatalytic surface. These results indicate that the metal complex is more stable than the ligand and the salt due to the fast electron movement and the superior effective surface area of the complex on the electrode surface [35]. The peak-peak separation values for the different electrodes (poly($Na_3[Cr(HR)_4Cl_2]$)/GCE, electrodeposited Cr(III)/GCE, and poly(NaHR)/GCE) are also provided, indicating the relative potential differences during the redox process. The largest peak-peak separation is observed for the poly($Na_3[Cr(HR)_4Cl_2]$)/GCE, followed by the electrodeposited Cr(III)/GCE, and finally the poly(NaHR)/GCE.

In general, poly($Na_3[Cr(HR)_4Cl_2]$)/GCE has a higher potential gap and greater stability compared to its ligand and $CrCl_3.6H_2O$ salt. The potential changes during the redox process are smaller for the complex compared to the ligand, and the complex exhibits a larger potential difference compared to the salt.

3.4.2. Charge transfer kinetics

To investigate the electrical characteristics of the interface between the modified electrode surface and the electrolyte, the charge transfer kinetics such as double layer capacitor and conductivity of the fabricated coordination complex polymer were examined. The Electrochemical impedance spectroscopy (EIS) technique was employed to characterize the conductivity of the bare GCE, poly(NaHR)/GCE, poly(Cr(0))/GCE, and poly($Na_3[Cr(HR)_4Cl_2]$)/GCE.

Fig. 4 illustrates the EIS results, showing a decreasing semicircle region for the poly($Na_3[Cr(HR)_4Cl_2]$)/GCE in comparison with the bare GCE, electrodeposited Cr(0)/GCE, and poly(NaHR)/GCE [36]. This indicates a significant improvement in the conductivity of the surface, tending to a faster electron transfer pathway between the analyte and
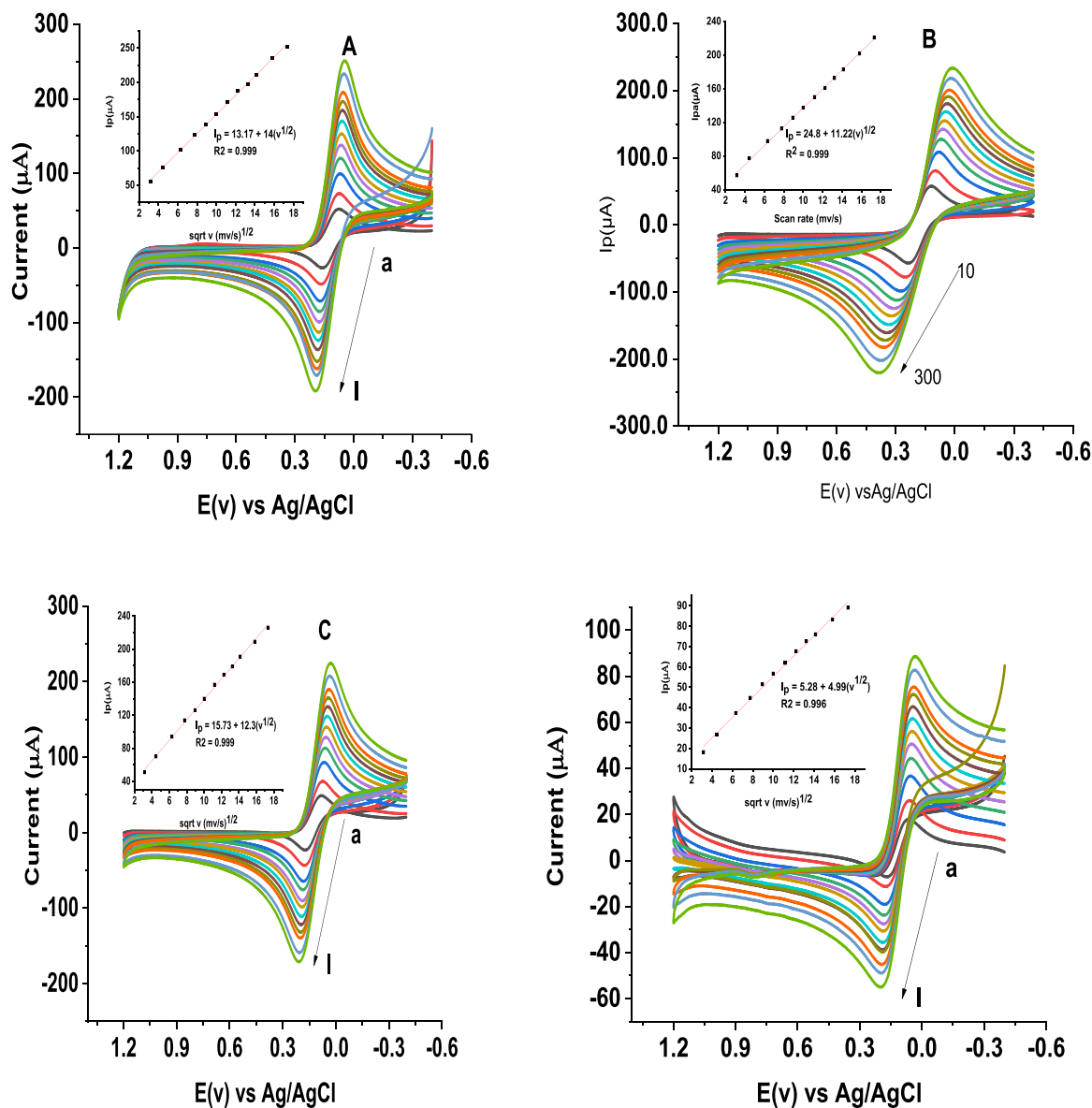
Fig. 2. Cyclic voltammograms of poly($Na_3[Cr(HR)_4Cl_2]$)/GCE (A), electrodeposited Cr(0)/GCE (B), poly(NaHR)/GCE (C), and bare GCE (D) in pH 7.0 PBS with 10.0 mM $Fe(CN)_6^{3-/4-}$ at different scan rates. Inset: corresponding plot of oxidative peak current vs. square root of scan rate.

Table 1

Summary of the comparison of the area of the precursor and complex modified electrodes.

Electrode	The slope of I_{pa} vs. $(v)^{1/2}$	Effective surface area $(cm)^2$
Unmodified GCE	4.99	0.069
Cr(0)/GCE	11.2	0.15
Poly(NaHR)/GCE	12.3	0.17
Poly($Na_3[Cr(HR)_4Cl_2]$)/GCE	14.0	0.2

the electrode surface.

The charge transfer resistance (Rct) value of the synthesized complex (Fig. 4 curve a), are more shifted to lower voltage compared to the free ligand, $CrCl_3 \cdot 6H_2O$, and unmodified GCE (curve d). This suggests that the modified complex has an enhanced conductivity because of the lower charge transfer resistance. The increased surface area (Fig. 2) and improved conductivity of the complex contribute to this reduction in

charge transfer resistance compared to the bare GCE [36]. The small semicircle diameter observed for poly($Na_3[(Cr(HR)_4Cl_2]$)/GCE indicates low charge transfer resistance, suggesting that the electrode is efficient at transferring charge across the interface.

Based on above findings, the synthesized complex is considered as a good conducting material. Its properties make it suitable for potential applications in sensors and catalysis, where efficient and fast electron transfer is required.

4. Antibacterial activities

The antibacterial activities of the ligand, salt, and complex were conducted on two Gram-positive bacteria (*S. aureus* and *S. epidermidis*) and two Gram-negative bacteria (*E. coli* and *K. pneumoniae*) on Muller-Hinton agar media and tetracycline as a standard drug. The complex showed improved and better antibacterial activities than the ligand and salt ranging from 30 ± 1.00 to 37.67 ± 1.15 mm (Fig. S3, Table 2, **and** Fig. S4). The enhanced in antibacterial activity of the complex can be explained on the basis of Overtone's concept [37] and Tweedy's
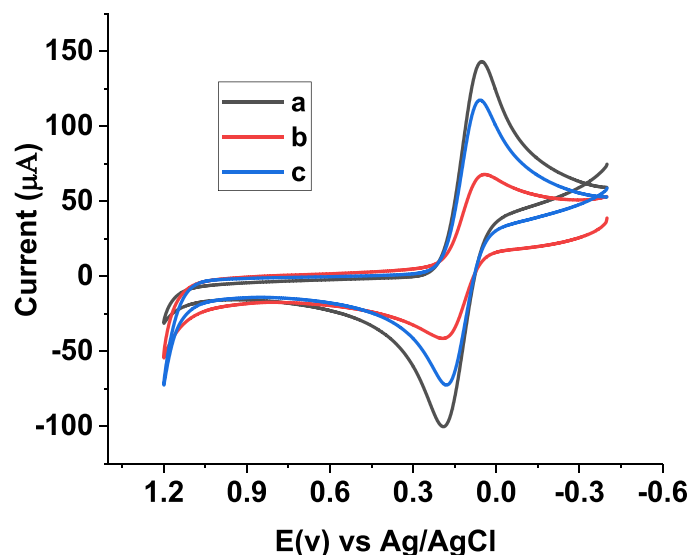
Fig. 3. CVs of 10.0 mM $Fe(CN)_6^{3-/4-}$ in 0.1 M KCl at poly($Na_3[Cr(HR)_4Cl_2]$)/GCE (curve a), poly(NaHR)/GCE (curve b), and electrodeposited Cr(0) (curve c) at the scan rate of 100 mV s^{-1}.
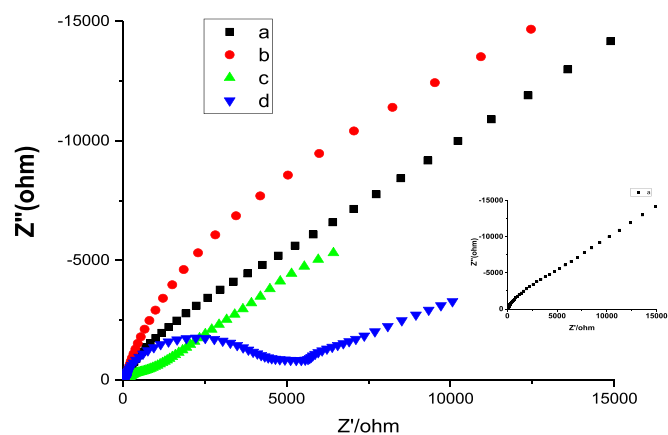

Fig. 4. Nyquist plot of poly($Na_3[Cr(HR)_4Cl_2]$)/GCE (a), electrodeposited Cr(0)/ GCE (b), poly(NaHR)/GCE (c), bare GCE (d), in pH 7.0 PBS with 10.0 mM [Fe $(CN)_6]^{3-/4-}$ and 0.1 M KCl in the frequency range: 0.01–50,000 Hz, amplitude: 0.01 V, and potential: 0.23 V.

chelation theory [38]. However, the complex exhibited lower antibacterial effects compared to the positive reference (a commercial antibiotic (tetracycline)) (Table S1). This could be due to the octahedral shape of the compound, which made it more difficult for it to penetrate the bacterial cell membrane and cell wall compared to the almost flat structure of the reference compound.

5. Conclusions

In summary, the newly synthesized anionic complex, is exhibiting several advantages over the resorcinolate ligand and $CrCl_3.6H_2O$ salt. It displayed a higher potential gap and greater stability. Moreover, poly ($Na_3[Cr(HR)_4Cl_2]$)/GCE demonstrated the highest electroactive effective surface area compared to the unmodified GCE, Cr(0)/GCE, and poly (NaHR)/GCE, along with low charge transfer resistance. This significant increase in the electroactive surface area of the modified electrode indicates the formation of a larger number of available electrochemical active sites on the surface of poly($Na_3(Cr(HR)_4Cl_2]$)/GCE, providing a

Table 2
Antibacterial activity of chromium salt, ligands, metal complex and the reference antibiotic in liquid phase.

N⁰	Sample and reference	Antimicrobial activity (mean IZ diameter (mm) $\pm$ SD)			
		Gram negative bacteria		Gram positive bacteria	
		E. coli	*K. Pneumonia*	*S. aureus*	*S. epidermidis*
1	$Na_3[Cr(HR)_4Cl_2]$	37.67 $\pm$ 1.15	33.33 $\pm$ 2.08	30 $\pm$ 1.00	31 $\pm$ 1.00
2	$CrCl_3\cdot6H_2O$	20.67 $\pm$ 1.15	22 $\pm$ 1.00	20 $\pm$ 1.00	20 $\pm$ 2.00
3	NaHR	26.67 $\pm$ 0.58	30 $\pm$ 1.00	28.67 $\pm$ 0.58	28.67 $\pm$ 0.58
4	Tetracycline	40.33 $\pm$ 0.58	40 $\pm$ 1.00	40.67 $\pm$ 0.58	39.67 $\pm$ 1.53
5	Solvent	0.00 $\pm$ 0.00	0.00 $\pm$ 0.00	0.00 $\pm$ 0.00	0.00 $\pm$ 0.00

The minimum inhibition concentrations (MIC) of the complex are 25 μg/mL on *E. coli*, and *S. epidermidis*, 50 μg/mL *K. pneumoniae* and 100 μg/mL on *S. aureus* (Table S2). $Na_3[Cr(HR)_4Cl_2]$ displayed MIC values of 25 ppm for *E. coli* and *S. epidermidis*, 50 ppm for *K. pneumoniae*, and 100 ppm for *S. aureus* (Table S2).

larger electrocatalytic surface.

Based on these findings, the synthesized complex can be considered as a highly conductive material suitable for potential applications in sensors and catalysis, especially in situations that require efficient and rapid electron transfer.

Additionally, $Na_3[Cr(HR)_4Cl_2]$ exhibited antibacterial activity against all tested pathogenic bacteria. The synthesised compound was able to interact with bacterial membranes and generate reactive oxygen species (ROS) by its redox-activities, ultimately causing damage to bacterial cells and exhibiting antibacterial activity, where fast electron transfer is required.

CRediT authorship contribution statement

Getinet Tamiru: Writing – review & editing, Supervision, Resources, Project administration, Investigation, Data curation. **Atakilt Abebe:** Writing – review & editing, Supervision, Resources, Project administration, Investigation, Data curation. **Wolfgang Linert:** Writing – original draft, Supervision, Project administration, Investigation, Data curation. **Tigist Tsega:** Writing – original draft, Methodology, Investigation, Formal analysis, Data curation, Conceptualization. **Madhu Thomas:** Writing – review & editing, Supervision, Project administration, Investigation, Data curation. **Adane Kassa:** Writing – original draft, Methodology, Investigation, Formal analysis, Conceptualization. **Getasil Chane:** Writing – original draft, Methodology, Investigation, Formal analysis, Data curation, Conceptualization. **Dawit Tesfaye:** Writing – original draft, Methodology, Investigation, Formal analysis, Conceptualization. **Mamo Gebrezgiabher:** Writing – original draft, Methodology, Investigation, Formal analysis, Conceptualization. **Mamaru Bitew:** Writing – original draft, Methodology, Investigation, Formal analysis, Conceptualization. **Melaku Motto:** Writing – original draft, Methodology, Investigation, Formal analysis, Conceptualization.

Acknowledgments

Declaration of Competing Interest

There are no conflicts to declare with regard to publishing this work.

Appendix A. Supporting information

Supplementary data associated with this article can be found in the online version at doi:10.1016/j.ijoes.2024.100659.

References

[1] A. Abebe, T. Hailemariam, Synthesis and assessment of antibacterial activities of ruthenium(III) mixed ligand complexes containing 1,10-phenanthroline and guanide, Bioinorg. Chem. Appl. 2016 (2016) 1–10, https://doi.org/10.1155/2016/3607924.

[2] B. Rosenberg, L. Van Camp, T. Krigas, Inhibition of cell division in Escherichia coli by electrolysis products from a platinum electrode [17], Nature 205 (1965) 698–699, https://doi.org/10.1038/205698a0.

[3] K. Kasemodel, K. Roberts, Metal-based chemotherapy drugs, Proc. Okla. Acad. Sci. 99 (2019) 106–113.

[4] G.A. Edwards, A.J. Bergren, M.D. Porter, Chemically modified electrodes, in: C. G. Zoski (Ed.), Handb. Electrochem., Elsevier, Amsterdam, Netherlands, 2007, pp. 295–327, https://doi.org/10.1016/B978-044451958-0.50021-5.

[5] K. Ghosh, P. Kumar, I. Goyal, Synthesis and characterization of chromium(III) complexes derived from tridentate ligands: generation of phenoxyl radical and catalytic oxidation of olefins, Inorg. Chem. Commun. 24 (2012) 81–86, https://doi.org/10.1016/j.inoche.2012.07.028.

[6] A.C. González-Baró, R. Pis-Diez, O.E. Piro, B.S. Parajón-Costa, Crystal structures, theoretical calculations, spectroscopic and electrochemical properties of Cr(III) complexes with dipicolinic acid and 1,10-phenantroline, Polyhedron 27 (2008) 502–512, https://doi.org/10.1016/j.poly.2007.10.005.

[7] R. Gusmão, Z. Sofer, M. Pumera, Metal phosphorous trichalcogenides (MPCh3): from synthesis to contemporary energy challenges, Angew. Chem. - Int. Ed. 58 (2019) 9326–9337, https://doi.org/10.1002/anie.201810309.

[8] M. Hecht, F.A. Schultz, B. Speiser, Ligand structural effects on the electrochemistry of chromium(III) amino carboxylate complexes, Inorg. Chem. 35 (1996) 5555–5563, https://doi.org/10.1021/ic960152o.

[9] A.R. Freitas, M. Silva, M.L. Ramos, L.L.G. Justino, S.M. Fonseca, M.M. Barsan, C.M. A. Brett, M.R. Silva, H.D. Burrows, Synthesis, structure, and spectral and electrochemical properties of chromium(iii) tris-(8-hydroxyquinolinate), Dalton Trans. 44 (2015) 11491–11503, https://doi.org/10.1039/c5dt00727e.

[10] S. Praveen Kumar, R. Suresh, K. Giribabu, R. Manigandan, S. Munusamy, S. Muthamizh, V. Narayanan, Synthesis and characterization of chromium(III) Schiff base complexes: antimicrobial activity and its electrocatalytic sensing ability of catechol, Spectrochim. Acta - Part A Mol. Biomol. Spectrosc. 139 (2015) 431–441, https://doi.org/10.1016/j.saa.2014.12.012.

[11] A. Kechiche, T. Fradi, O. Noureddine, M. Guergueb, F. Loiseau, V. Guerineau, N. Issoui, A. Lemeune, H. Nasri, Synthesis, characterization and catalytic studies of chromium(III) porphyrin complex with axial cyanate ligands, J. Mol. Struct. 1250 (2022) 1–43, https://doi.org/10.1016/j.molstruc.2021.131801.

[12] M.C. Vlasiou, K.S. Pafiti, Chromium coordination compounds with antimicrobial activity: synthetic routes, structural characteristics, and antibacterial activity, Open Med. Chem. J. 14 (2020) 1–25, https://doi.org/10.2174/1874104502014010001.

[13] R.A. Murcia, S.M. Leal, M.V. Roa, E. Nagles, A. Muñoz-Castro, J.J. Hurtado, Development of antibacterial and antifungal triazole chromium(III) and cobalt(II) complexes: synthesis and biological activity evaluations, Molecules 23 (2018) 1–16, https://doi.org/10.3390/molecules23082013.

[14] D.P. Singh, K. Kumar, C. Sharma, Antimicrobial active macrocyclic complexes of Cr (III), Mn(III) and Fe(III) with their spectroscopic approach, Eur. J. Med. Chem. 44 (2009) 3299–3304, https://doi.org/10.1016/j.ejmech.2009.02.029.

[15] D.A. Siéwé, E.S. Fondjo, J.D.D. Tamokou, S.E. Ekom, K.S.D. Dimo, G. Doungmo, M. E. Walters, A. Tsopmo, P.F.W. Simon, J.R. Kuiate, Chromium (III) complex of 2-amino-3-carbomethoxy-4,5,6,7-tetrahydrobenzo[B] thiophene: synthesis, characterization and antimicrobial activity, J. Chil. Chem. Soc. 65 (2020) 4908–4913, https://doi.org/10.4067/s0717-97072020000204908.

[16] A. Levina, P.A. Lay. Redox Chemistry and Biological Activities of Chromium(III) Complexes, Second Edi, Elsevier B.V., 2019, https://doi.org/10.1016/b978-0-444-64121-2.00009-x.

[17] P. Cui, Z. Cheng, J. Sun, Effects of different chromium sources on growth performance, serum biochemical, hepatopancreas glycometabolism enzymes activities, IR, GLUT2 and SGLT1 gene expression of common carp (Cyprinus carpio), Aquac. Res. 53 (2022) 1573–1581, https://doi.org/10.1111/are.15692.

[18] A. Monga, A.B. Fulke, D. Dasgupta, Recent developments in essentiality of trivalent chromium and toxicity of hexavalent chromium: implications on human health and remediation strategies, J. Hazard. Mater. Adv. 7 (2022) 100113, https://doi.org/10.1016/j.hazadv.2022.100113.

[19] J. long Dong, B. Wen, Z. Song, J. Chai, B. Liu, W. juan Tian, G. Liang, B. sheng Yang, Potential antidiabetic molecule involving a new chromium(III) complex of dipicolinic and metformin as a counter ion: synthesis, structure, spectroscopy, and bioactivity in mice, Arab. J. Chem. 14 (2021) 103236, https://doi.org/10.1016/j.arabjc.2021.103236.

[20] S. Rastegarnia, M. Pordel, S. Allameh, Synthesis, characterization, antibacterial studies and quantum-chemical investigation of the new fluorescent Cr(III) complexes, Arab. J. Chem. 13 (2020) 3903–3909, https://doi.org/10.1016/j.arabjc.2019.03.001.

[21] Y. Liu, A. Cotillard, C. Vatier, J.P. Bastard, S. Fellahi, M. Stévant, O. Allatif, C. Langlois, S. Bieuvelet, A. Brochot, A. Guilbot, K. Clément, S.W. Rizkalla, A dietary supplement containing cinnamon, chromium and carnosine decreases fasting plasma glucose and increases lean mass in overweight or obese pre-diabetic subjects: a randomized, placebo-controlled trial, PLoS One 10 (2015) 1–21, https://doi.org/10.1371/journal.pone.0138646.

[22] P. Whitfield, A. Parry-Strong, E. Walsh, M. Weatherall, J.D. Krebs, The effect of a cinnamon-, chromium- and magnesium-formulated honey on glycaemic control, weight loss and lipid parameters in type 2 diabetes: an open-label cross-over randomised controlled trial, Eur. J. Nutr. 55 (2016) 1123–1131, https://doi.org/10.1007/s00394-015-0926-x.

[23] A.I. Vogel, A Textbook of Quantitative Inorganic Analysis, third edit, Longman, London and New york, 1961.

[24] W.J. Geary, The use of conductivity measurements in organic solvents for the characterisation of coordination compounds, Coord. Chem. Rev. 7 (1971) 81–122, https://doi.org/10.1016/S0010-8545(00)80009-0.

[25] K. Nakamoto, Infrared and raman spectra of inorganic and coordination compounds, in: Infrared Raman Spectra Inorg. Coord. Compd., John Wiley & Sons, Ltd., Marquette University, Milwaukee, WI, USA, 1978, pp. 1357–1363, https://doi.org/10.1016/s0022-328x(00)93553-8.

[26] A.B.P. Lever, Inorganic Electronic Spectroscopy, Tokyo Elsevier, Amsterdam, 1984 (Amsterdam, Oxford, New York).

[27] E.L.A. Eftimie, N.M. Avram, Absorption spectra, ligand field parameters and g factors of Cr^{3+} doped α-Al2O3 laser crystal: ab initio calculations, Phys. Scr. 95 (2020) 44005, https://doi.org/10.1088/1402-4896/ab60fc.

[28] M. Amare, S. Aklog, Electrochemical determination of caffeine content in ethiopian coffee samples using lignin modified glassy carbon electrode, J. Anal. Methods Chem. 2017 (2017), https://doi.org/10.1155/2017/3979068.

[29] M. Gashu, B.A. Aragaw, M. Tefera, A. Abebe, Poly(bis(2,2'-bipyridine) hydroxy Copper(II) iodide modified glassy carbon electrode for electrochemical determination of chloroquine in pharmaceuticals and biological samples, Sens. Bio-Sens. Res. 42 (2023) 100598, https://doi.org/10.1016/j.sbsr.2023.100598.

[30] A. Kassa, A. Abebe, G. Tamiru, M. Amare, Synthesis of a novel [diresorcinate-1,10-phenanthrolinecobalt(II)] complex, and potentiodynamic fabrication of poly (DHRPCo)/GCE for selective square wave voltammetric determination of procaine penicillin G in pharmaceutical and biological fluid samples, ChemistrySelect 7 (1) (2022) 19, https://doi.org/10.1002/slct.202103458.

[31] M. Gharous, L. Bounab, F.J. Pereira, M. Choukairi, R. López, A.J. Aller, Electrochemical kinetics and detection of paracetamol by stevensite-modified carbon paste electrode in biological fluids and pharmaceutical formulations, Int. J. Mol. Sci. 24 (2023), https://doi.org/10.3390/ijms241411269.

[32] N. Raeisi-Kheirabadi, A. Nezamzadeh-Ejhieh, H. Aghaei, Cyclic and linear sweep voltammetric studies of a modified carbon paste electrode with nickel oxide nanoparticles toward tamoxifen: effects of surface modification on electrode response kinetics, ACS Omega 7 (2022) 31413–31423, https://doi.org/10.1021/acsomega.2c03441.

[33] A. Debalke, A. Kassa, T. Asmellash, Y. Beyene, M. Amare, G.T. Tigineh, A. Abebe, Synthesis of a novel diaquabis(1,10-phenanthroline)copper(II)chloride complex and its voltammetric application for detection of amoxicillin in pharmaceutical and biological samples, Heliyon 8 (2022) e11199, https://doi.org/10.1016/j.heliyon.2022.e11199.

[34] D.M.R. de Rooij. Electrochemical Methods: Fundamentals and Applications, 2nd ed., John Wiley & Sons, 2003 https://doi.org/10.1108/acmm.2003.12850eae.001.

[35] S. Deepa, B.E.K. Swamy, K.V. Pai, A surfactant SDS modified carbon paste electrode as an enhanced and effective electrochemical sensor for the determination of doxorubicin and dacarbazine its applications: a voltammetric study, J. Electroanal. Chem. 879 (2020) 114748, https://doi.org/10.1016/j.jelechem.2020.114748.

[36] A. Kassa, A. Abebe, M. Amare, Synthesis, characterization, and electropolymerization of a novel Cu(II) complex based on 1,10-phenanthroline for electrochemical determination of amoxicillin in pharmaceutical tablet formulations, Electrochim. Acta 384 (2021) 138402, https://doi.org/10.1016/j.electacta.2021.138402.

[37] N. Dharmaraj, P. Viswanathamurthi, K. Natarajan, Ruthenium(II) complexes containing bidentate Schiff bases and their antifungal activity, Transit. Met. Chem. 26 (2001) 105–109, https://doi.org/10.1023/A:1007132408648.

[38] J.S. Sultan, S.M. Lateaf, D.K. Rashid, Synthesis, characterization and synthesis, characterization and antibacterial activity of mixed ligand (HL) complexes Mn(ll), Co(ll), Ni(ll), Zn(ll), Cd(ll) and Hg(ll) with azide (N3−), Open J. Inorg. Chem. 5 (2015) 102–111, https://doi.org/10.4236/ojic.2015.54011.